 doi:10.20944/preprints202205.0191.v1

Nonlinear analysis of beat-to-beat variability of action potential time series data identifies dynamic reentrant substrates in a hypokalaemic mouse model of acquired long QT syndrome

Running title: Non-linear repolarization variability and arrhythmias in hypokalaemia mouse model

Gary Tse MD PhD FRCP * [1, 2, 3], Jiandong Zhou * [4], Xiuming Dong MS [5], Guoliang Hao PhD [6,7], Sharen Lee MBChB [1], Keith Sai Kit Leung BSc [1], Tong Liu MD PhD [2], Yimei Du PhD [7], Shuk Han Cheng PhD [8], Wing Tak Wong PhD [9]

[1] Cardiac Electrophysiology Unit, Cardiovascular Analytics Group, Hong Kong, China-UK Collaboration
[2] Tianjin Key Laboratory of Ionic-Molecular Function of Cardiovascular Disease, Department of Cardiology, Tianjin Institute of Cardiology, Second Hospital of Tianjin Medical University, Tianjin 300211, China
[3] Kent and Medway Medical School, Canterbury, UK
[4] Nuffield Department of Medicine, University of Oxford, Oxford, UK
[5] Henan SCOPE Research Institute of Electrophysiology Co. Ltd., Kaifeng 475000, China
[6] Burdon Sanderson Cardiac Science Centre and BHF Centre of Research Excellence, Department of Physiology, Anatomy and Genetics, University of Oxford, Oxford OX1 3PT, UK
[7] Department of Cardiology, Union Hospital, Tongji Medical College, Huazhong University of Science and Technology, Wuhan, Hubei 430022, China
[8] Department of Biomedical Sciences, City University of Hong Kong, Tat Chee Avenue, Kowloon Tong, Hong Kong
[9] School of Life Sciences, Chinese University of Hong Kong, Hong Kong, China

* Joint first authors and equal contributors

Correspondence to

Prof. Shuk Han Cheng, PhD
Department of Biomedical Sciences,
City University of Hong Kong,
Tat Chee Avenue, Kowloon Tong, Hong Kong, China
Email: bhcheng@cityu.edu.hk

Prof. Wing Tak Wong
School of Life Sciences,
The Chinese University of Hong Kong,
Hong Kong, China
Email: jack_wong@cuhk.edu.hk

 doi:10.20944/preprints202205.0191.v1

Abstract

Background: Previous studies have quantified repolarization variability using time-domain, frequency-domain and non-linear analysis in mouse hearts. Here, we investigated the relationship between these parameters and ventricular arrhythmogenicity in a hypokalaemia model of acquired long QT syndrome.

Methods: Left ventricular monophasic action potentials (MAPs) were recorded during right ventricular regular 8 Hz pacing during normokalaemia (5.2 mM [K^+]), hypokalaemia modelling LQTS (3 mM [K^+]) or hypokalaemia with 0.1 mM heptanol in Langendorff-perfused mouse hearts.

Results: During normokalaemia, mean APD was 33.5±3.7 ms. Standard deviation (SD) of APDs was 0.63±0.33 ms, coefficient of variation was 1.9±1.0% and the root mean square (RMS) of successive differences in APDs was 0.3±0.1 ms. Low- and high-frequency peaks were 0.6±0.5 and 2.3±0.7 Hz, respectively, with percentage powers of 38±22 and 61±23%. Poincaré plots of APD_{n+1} against APD_n revealed ellipsoid morphologies with SD along the line-of-identity (SD2) to SD perpendicular to the line-of-identity (SD1) ratio of 4.6±1.1. Approximate and sample entropy were 0.49±0.12 and 0.64±0.29, respectively. Detrended fluctuation analysis revealed short- and long-term fluctuation slopes of 1.62±0.27 and 0.60±0.18, respectively. Hypokalaemia provoked ventricular tachycardia in six of seven hearts, prolonged APDs (51.2±7.9 ms), decreased SD2/SD1 ratio (3.1±1.0), increased approximate and sample entropy (0.68±0.08 and 1.02±0.33) and decreased short-term fluctuation slope (1.23 ± 0.20) (ANOVA, $P<0.05$). Heptanol prevented VT in all hearts studied without further altering the above repolarization parameters observed during hypokalaemia.

Conclusion: Reduced SD2/SD1, increased entropy and decreased short-term fluctuation slope are associated with ventricular arrhythmogenesis in hypokalaemia. Heptanol exerts anti-arrhythmic effects without affecting repolarization variability.

Word count: 250 words

 doi:10.20944/preprints202205.0191.v1

Keywords: repolarization variability; beat-to-beat; entropy; delayed repolarization; long QT

Introduction

Long QT syndrome (LQTS) is an important clinical condition predisposing to the development of life-threatening ventricular arrhythmias and sudden cardiac death. It can have congenital or acquired causes, the latter reflected by electrolyte disturbances such as hypokalemia or certain drugs that block potassium channels. Previously, several important re-entrant substrates of hypokalaemia have been identified using pre-clinical models [1-4]. These include repolarization abnormalities in the form of action potential prolongation, increased transmural dispersion of repolarization, reduced refractoriness, steep restitution gradients and increased amplitude of repolarization alternans [5, 6].

Moreover, altered beat-to-beat variations in the repolarization time-course have been associated with arrhythmogenesis in other pharmacological or disease models [7, 8]. For example, higher degrees of short-term repolarization variability using Poincaré plot analysis were associated with the development of ventricular arrhythmias in dogs [9]. Moreover, a combined experimental and computational approach associated higher repolarization variability with pro-arrhythmic abnormalities [10]. Finally, high entropy was shown to predict arrhythmic outcomes following gap junction and sodium channel inhibition in a mouse model [11]. However, whether variability or complexity of beat-to-beat repolarization variability plays a role in hypokalaemia modelling LQTS has never been studied. In this study, we tested the hypothesis that increased repolarization variability contributes to arrhythmic substrate in an experimental mouse model of LQTS using hypokalaemia.

Materials and Methods

Preprints (www.preprints.org) | NOT PEER-REVIEWED | Posted: 13 May 2022 doi:10.20944/preprints202205.0191.v1

This study received approval from the University of Cambridge (Approval Number: BB/G017565/1). The methodology used in this study has previously been described by us in detail, and is reproduced here with permission [11]:

Solutions

Krebs-Henseleit solution (composition in mM: NaCl 119, $NaHCO_3$ 25, KCl 4, KH_2PO_4 1.2, $MgCl_2$ 1, $CaCl_2$ 1.8, glucose 10 and sodium pyruvate 2, pH 7.4), which has been bicarbonate-buffered and bubbled with 95% O_2–5% CO_2, was used in the experiments described in this study. Heptanol (Sigma, Dorset, UK; density: 0.82 g ml^{-1}) is an agent that remains soluble in aqueous solutions up to 9 mM (The Merck Index, New Jersey, USA). Krebs-Henseleit solution was used to dilute the heptanol solution to produce a final concentration of 0.1 mM.

Preparation of Langendorff-perfused mouse hearts

This study was approved by the Animal Welfare and Ethical Review Body at the University of Cambridge. Wild-type mice of 129 genetic background between 5 and 7 months of age were used. They were maintained at room temperature (21 ± 1°C) and were subjected to a 12:12 h light / dark cycle with free access to sterile rodent chow and water in an animal facility. Mice were terminated by dislocation of the cervical spine in accordance with Sections 1(c) and 2 of Schedule 1 of the UK Animals (Scientific Procedures) Act 1986. After removal from their chest cavities, the hearts were submerged in ice-cold Krebs-Henseleit solution. The aortas were cannulated using a custom-made 21-gauge cannula prefilled with ice-cold buffer. A micro-aneurysm clip (Harvard Apparatus, UK) was used to secure the hearts onto the Langendorff perfusion system. Retrograde perfusion was carried out at a flow rate of 2 to 2.5 ml min^{-1} by use of a peristaltic pump (Watson–Marlow Bredel pumps model 505S, Falmouth, Cornwall, UK). The perfusate passed through successively 200 and 5 μm filters and warmed to 37°C using a water jacket and circulator before arriving at the aorta. Approximately 90%

Preprints (www.preprints.org) | NOT PEER-REVIEWED | Posted: 13 May 2022 doi:10.20944/preprints202205.0191.v1

of the hearts regained their pink colour and spontaneous rhythmic activity. These were therefore studied further. The remaining 10% did not and were discarded. The hearts were perfused for a further 20 minutes to minimise residual effects of endogenous catecholamine release, before their electrophysiology properties were characterized.

Stimulating and recording procedures

Paired platinum electrodes (1 mm interpole distance) were used to stimulate the right ventricular epicardium electrically. This took place at 8 Hz, using square wave pulses of 2 ms in duration, with a stimulation voltage set to three times the diastolic threshold (Grass S48 Stimulator, Grass-Telefactor, Slough, UK) immediately after the start of perfusion.

A monophasic action potential (MAP) electrode was used to record MAPs from the left ventricular epicardium (Linton Instruments, Harvard Apparatus). The stimulating and recording electrodes were maintained at constant positions separated approximately by distance of 3 mm. All recordings were performed using a baseline cycle length (BCL) of 125 ms (8 Hz) to exclude rate-dependent differences in action potential durations (APDs). MAPs were pre-amplified using a NL100AK head stage, amplified with a NL 104A amplifier and band pass filtered between 0.5 Hz and 1 kHz using a NL125/6 filter (Neurolog, Hertfordshire, UK) and then digitized (1401plus MKII, Cambridge Electronic Design, Cambridge, UK) at 5 kHz. Waveforms were analysed using Spike2 software (Cambridge Electronic Design, UK). MAP waveforms that did not match established criteria for MAP signals were rejected [12, 13]. They must have stable baselines, fast upstrokes, with no inflections or negative spikes, and a rapid first phase of repolarization. 0% repolarization was measured at the peak of the MAP and 100% repolarization was measured at the point of return of the potential to baseline [12, 14, 15].

Preprints (www.preprints.org) | NOT PEER-REVIEWED | Posted: 13 May 2022 doi:10.20944/preprints202205.0191.v1

APD variability analysis

APD variability analysis was performed using Kubios HRV Standard software (Version 3.0.2) over a 20-second period. Time-domain analysis yielded the 1) standard deviation (SD) of APDs, which represents the overall (short-term and long-term) variability, and 2) root mean square (RMSSD) of successive differences of APDs, which represents the short-term variability:

$$\text{SDAPD} = \sqrt{\frac{1}{N-1}\sum_{j=1}^{N}(\text{APD}_j - \overline{\text{APD}})^2}$$

$$\text{RMSSD} = \sqrt{\frac{1}{N-1}\sum_{j=1}^{N-1}(\text{APD}_{j+1} - \text{APD}_j)^2}$$

Frequency-domain analysis was conducted using the Fast Fourier Transform method. For frequency domain parameters, spectral analysis was performed by using fast-Fourier transform method. The sampling frequency was set to 8 Hz. The power in the repolarization spectrum between 0.04 and 4 Hz was defined as total power (TP). The power in the repolarization spectrum was divided into three different frequency bands: very low frequency power (VLF, 0 to 0.04 Hz), low frequency power (LF, 0.04 to 1.5 Hz) and high frequency power (HF, 1.5 to 4 Hz).

Non-linear properties of APD variability were studied as follow. Poincaré plots are graphical representations of the correlation between successive APD values, in which APD_{n+1} is plotted against APD_n. This enables determination of the SD of the points perpendicular to the line-of-identity (SD1), which describes the short-term variability, and the SD of the points along the line-of-identity (SD2), which describes the long-term variability. The ratio SD2 to SD1 then gives an indication of the degree of long-term variability in relation to the short-term variability. The approximate entropy provides a measure of the irregularity of the signal. It is computed as follows:

Firstly, a set of length m vectors u_j is formed:

Preprints (www.preprints.org) | NOT PEER-REVIEWED | Posted: 13 May 2022 doi:10.20944/preprints202205.0191.v1

$u_j = (APD_j ; APD_{j+1},\ldots, APD_{j+m-1}); j = 1; 2; \ldots N - m + 1$

where m is the embedding dimension and N is the number of measured APDs. The distance between these vectors is defined as the maximum absolute difference between the corresponding elements:

$d(u_j, u_k) = \max \{|APD_{j+n} - APD_{k+n}| \mid n=0, \ldots, m-1\}$

for each u_j the relative number of vectors u_k for which $d(u_j, u_k) \leq r$ is calculated. This index is denoted with Cmj (r) and can be written in the form

$$C_j^m(r) = \frac{\text{nbr of } \{u_k \mid d(u_j, u_k) \leq r\}}{N - m + 1} \quad \forall k.$$

Taking the natural logarithms gives:

$$\Phi^m(r) = \frac{1}{N - m + 1} \sum_{j=1}^{N-m+1} \ln C_j^m(r).$$

The approximate entropy is then defined as:

$$\text{ApEn}(m, r, N) = \Phi^m(r) - \Phi^{m+1}(r).$$

Lower approximate entropy values reflect a more regular signal, whereas higher values reflect a more irregular signal.

The sample entropy also provides a measure of signal irregularity but is less susceptible to bias than approximate entropy. This is given by:

$$C_j^m(r) = \frac{\text{nbr of } \{u_k \mid d(u_j, u_k) \leq r\}}{N - m} \quad \forall k \neq j.$$

Averaging gives:

$$C^m(r) = \frac{1}{N - m + 1} \sum_{j=1}^{N-m+1} C_j^m(r)$$

The sample entropy is then given by:

$$\text{SampEn}(m, r, N) = \ln (C^m(r)/C^{m+1}(r)).$$

Preprints (www.preprints.org) | NOT PEER-REVIEWED | Posted: 13 May 2022 doi:10.20944/preprints202205.0191.v1

Finally, detrended fluctuation analysis (DFA) was performed to determine long-range correlations in non-stationary physiological time series [16], yielding both short-term fluctuation (α1) and long-term fluctuation (α2) slopes. The point at which the slopes α1 and α2 meet is the crossover point.

Statistical analysis

All values were expressed as mean ± standard error of the mean (SEM). Numerical data were compared by one-way analysis of variance (ANOVA). $P < 0.05$ was considered statistically significant and was denoted by * in the figures.

Results

Action potential duration variability determined using time-domain methods

Our previous work has reported the pro-arrhythmic effects of hypokalaemia and anti-arrhythmic effects of 0.1 mM heptanol under hypokalaemic conditions [17]. This is an extension of the previously work by examining the beat-to-beat variability in repolarization durations of monophasic action potential (MAP) time series data over 20-second periods. Typical examples of MAP waveforms, time series and histograms of action potential durations (APDs) at 90% repolarization for normokalaemia**,** hypokalemia alone or in the presence of 0.1 mM heptanol are shown in **Figure 1A, Figure 1B** and **Figure 1C**, respectively. Time-domain analysis demonstrated a mean APD_{90} of 33.5 ± 3.7 ms (**Figure 2A**), standard deviation (SD) of APDs of 0.63 ± 0.33 ms (**Figure 2B**), coefficient of variation (CoV) of 1.9 ± 1.0% (**Figure 2C**), and root mean square (RMS) of successive differences in APDs of 0.3 ± 0.1 ms (**Figure 2D**). Hypokalemia prolonged APD_{90} to 51.2 ± 7.9 ms without significantly altering the remaining parameters (ANOVA, $P > 0.05$). After further treatment with heptanol, all of the above parameters remained unaltered (ANOVA, $P > 0.05$).

Preprints (www.preprints.org) | NOT PEER-REVIEWED | Posted: 13 May 2022 doi:10.20944/preprints202205.0191.v1

Action potential duration variability determined using frequency-domain methods

Fast Fourier Transform was used to generate frequency spectra, with examples obtained during normokalaemia, hypokalemia alone or in the presence of 0.1 mM heptanol are shown in **Figures 3A to 3C**. Frequency-domain analysis revealed that the peaks for very low-, low- and high-frequency were 0.03 ± 0.01, 0.58 ± 0.46 and 2.30 ± 0.74 Hz, respectively (**Figures 4A to C**). Their corresponding powers took values of 0.00 ± 0.01, 0.22 ± 0.28 and 0.23 ± 0.18 ms^2, respectively (**Figures 4D to F**). The low-frequency to high-frequency ratio was 0.95 ± 0.98 (**Figures 4G**) and total power (in log units) was –1.25 ± 1.11 (**Figures 4H**). Their percentage powers were 1.2 ± 2.0, 38.3 ± 22.4 and 60.5 ± 23.5% (**Figures 4I to K**). None of these parameters was altered by hypokalemia alone or in the presence of 0.1 mM heptanol (ANOVA, $P > 0.05$).

Action potential duration variability determined using non-linear methods

Poincaré plots expressing APD_{n+1} as a function of APD_n were constructed (**Figure 5A to 5C**). In all of the hearts studied, ellipsoid shapes of the data points were observed. The SD perpendicular to the line-of-identity (SD1), SD along the line-of-identity (SD2) and the SD2/SD2 ratio are shown in **Figures 6A to 6C**, taking values of 0.19 ± 0.08, 0.87 ± 0.46 and 4.60 ±1.07, respectively. Approximate and sample entropy were 0.49 ± 0.12 (**Figure 6D**) and 0.64 ± 0.29, respectively (**Figure 6E**). Detrended fluctuation analysis plotting the detrended fluctuations F(n) as a function of n in a log-log scale was performed (**Figure 7A to 8C**). This revealed short- and long-term fluctuation slopes of 1.62 ± 0.27 (**Figure 7D**) and 0.60 ± 0.18 (**Figure 7E**), respectively. Hypokalemia significantly decreased SD2/SD1 ratio to 3.1±1.0, increased approximate and sample entropy to 0.68 ± 0.08 and 1.02 ± 0.33 and decreased short-term fluctuation slope to 1.23 ± 0.20 (ANOVA, $P < 0.05$). After treatment with heptanol, no further changes in the above parameters were observed (ANOVA, $P > 0.05$).

Preprints (www.preprints.org) | NOT PEER-REVIEWED | Posted: 13 May 2022 doi:10.20944/preprints202205.0191.v1

Discussion

In this study, we examined the effects of experimental hypokalemia modelling acquired long QT syndrome on beat-to-beat variability in APD using time-domain, frequency-domain and non-linear analyses. Our main findings are that 1) increased arrhythmogenicity in hypokalemia was associated with prolonged APD, decreased SD2/SD1 ratio, increased approximate and sample entropy, and a decrease in short-term fluctuation slope; 2) heptanol exerted anti-arrhythmic effects despite leaving the hypokalemia-induced repolarization abnormalities unaltered.

Beat-to-beat variability in repolarization time-courses is a normal physiological phenomenon reflecting stochastic fluctuations in ion channel gating. Previous reports demonstrate that this variability is altered in pro-arrhythmic states. For example, higher degree of short-term variability determined using the Poincaré method was detected before the occurrence of *torsade de pointes* with reduced intercellular coupling in a canine model [9]. Secondly, computational modelling efforts complemented by experimental data suggested that higher variability was associated with pro-arrhythmic abnormalities using similar Poincaré plots [10]. Such a temporal variability in repolarization provide incremental value for arrhythmic risk stratification in human subjects with non-ischemic heart failure [18]. Recently, our group reported the use of time-domain, frequency-domain and fractal complexity analysis for assessing repolarization variability of action potential waveforms recorded from mouse hearts [19]. This was subsequently extended to demonstrations that non-linear measures of repolarization variability, such as SD2/SD1, entropy, and fluctuation slope can predict ventricular arrhythmogenesis in mouse hearts using the gap junction and sodium channel blocker, heptanol [11]. The present work extends these findings by demonstrating that such measures of repolarization variability can similarly reveal reentrant substrate in the context of acquired LQTS and represent biomarkers that can improve risk stratification. These findings have clinical implications given recent demonstrations of the association between increased beat-to-beat variability in the electrocardiographic T-wave with

 doi:10.20944/preprints202205.0191.v1

sudden cardiac death [20], but it remains to be elucidated whether the non-linear measures would predict ventricular arrhythmias or sudden cardiac death in the clinical setting [21].

Previous studies have reported alterations in beat-to-beat repolarization variability with differing degrees of gap junction coupling using time-domain methods. Thus, single ventricular cardiomyocytes isolated from canine hearts showed a baseline level of APD variability [22]. When two cardiomyocytes were electrically coupled, this variability was attenuated [22]. These experimental findings were supported of those from computational modelling studies, reporting higher repolarization variability with lower level of intercellular coupling [23]. In the present work, APD variability was not significantly higher after introduction of heptanol. Some possible reasons could explain the present findings. For example, heptanol has multiple targets, such as potassium and calcium channels [8]. It was previously demonstrated that beat-to-beat variability is affected by not only the mean APD but also the pacing rate [24]. Future studies should explore the relationship between pacing rate and the measures of variability examined in this study.

Our findings in the mouse are in keeping with those from clinical studies. In heart failure patients, higher approximate entropy of the interval between R_{peak} and T_{peak} were predictive of appropriate ICD shocks and death [25]. Moreover, in patients who have implantable cardioverter-defibrillator for primary prevention, high entropy of QT intervals also predicted ventricular arrhythmogenesis and mortality [26]. This study extends these findings by quantifying entropy using action potential time-series data recorded from isolated hearts that are free from autonomic influence and associated increased entropy with ventricular arrhythmogenesis under hypokalaemic conditions. Interestingly, our study found that it was possible to reduce arrhythmogenicity in the presence of high variability in beat-to-beat repolarization. Instead, the anti-arrhythmic effects are instead attributed to increases in tissue refractoriness, which was initially reduced by hypokalemia [17]. These findings are in keeping with known effects of different anti-arrhythmic agents. For example, class III and class IV anti-arrhythmic agents inhibit potassium and calcium channels, respectively, yet they increase beat-to-beat variability

 doi:10.20944/preprints202205.0191.v1

for two reasons. Firstly, the inward calcium current has the highest amplitude at the beginning of the plateau phase of cardiac repolarization, and this is a powerful modulator of subsequent potassium channel activation [27]. Secondly, the membrane resistance is high during the late phase of repolarization [22], and any small increase in the net inward current (e.g. produced by potassium channel block) can lead to larger variation in APD [28, 29]. Together, these findings would suggest multiple interacting mechanisms that are important determinants of arrhythmogenesis.

Conclusions

Reduced SD2/SD1 and increased entropy and decreased short-term fluctuation slope are associated with ventricular arrhythmogenesis in hypokalaemia. Heptanol exerts anti-arrhythmic effects without significantly influencing repolarization variability.

Acknowledgements

GT received research funding from the BBSRC from the UK for this research. WTW is supported by the Direct Grant for Research from the Research Committee of the Chinese University of Hong Kong, China.

Conflicts of Interest

None declared.

Funding

BBSRC.

 doi:10.20944/preprints202205.0191.v1

References

1. Tse G, Li KHC, Cheung CKY, Letsas KP, Bhardwaj A, Sawant AC, Liu T, Yan GX, Zhang H, Jeevaratnam K, Sayed N, Cheng SH and Wong WT. Arrhythmogenic Mechanisms in Hypokalaemia: Insights From Pre-clinical Models. *Front Cardiovasc Med*. 2021;8:620539.
2. Osadchii OE. Mechanisms of hypokalemia-induced ventricular arrhythmogenicity. *Fundam Clin Pharmacol*. 2010;24:547-59.
3. Weiss JN, Qu Z and Shivkumar K. Electrophysiology of Hypokalemia and Hyperkalemia. *Circ Arrhythm Electrophysiol*. 2017;10.
4. Gurung B, Tse G, Keung W, Li RA and Wong WT. Arrhythmic Risk Assessment of Hypokalaemia Using Human Pluripotent Stem Cell-Derived Cardiac Anisotropic Sheets. *Front Cell Dev Biol*. 2021;9:681665.
5. Tse G, Wong ST, Tse V and Yeo JM. Restitution analysis of alternans using dynamic pacing and its comparison with S1S2 restitution in heptanol-treated, hypokalaemic Langendorff-perfused mouse hearts. *Biomed Rep*. 2016;4:673-680.
6. Osadchii OE. Effects of ventricular pacing protocol on electrical restitution assessments in guinea-pig heart. *Exp Physiol*. 2012;97:807-21.
7. Couderc JP. Cardiac regulation and electrocardiographic factors contributing to the measurement of repolarization variability. *J Electrocardiol*. 2009;42:494-9.
8. Nanasi PP, Magyar J, Varro A and Ordog B. Beat-to-beat variability of cardiac action potential duration: underlying mechanism and clinical implications. *Can J Physiol Pharmacol*. 2017;95:1230-1235.
9. Thomsen MB, Verduyn SC, Stengl M, Beekman JD, de Pater G, van Opstal J, Volders PG and Vos MA. Increased short-term variability of repolarization predicts d-sotalol-induced torsades de pointes in dogs. *Circulation*. 2004;110:2453-9.
10. Pueyo E, Corrias A, Virag L, Jost N, Szel T, Varro A, Szentandrassy N, Nanasi PP, Burrage K and Rodriguez B. A multiscale investigation of repolarization variability and its role in cardiac arrhythmogenesis. *Biophys J*. 2011;101:2892-902.
11. Tse G, Hao G, Lee S, Zhou J, Zhang Q, Du Y, Liu T, Cheng SH and Wong WT. Measures of repolarization variability predict ventricular arrhythmogenesis in heptanol-treated Langendorff-perfused mouse hearts. *Curr Res Physiol*. 2021;4:125-134.
12. Knollmann BC, Katchman AN and Franz MR. Monophasic action potential recordings from intact mouse heart: validation, regional heterogeneity, and relation to refractoriness. *J Cardiovasc Electrophysiol*. 2001;12:1286-1294.
13. Tse G, Wong ST, Tse V and Yeo JM. Monophasic action potential recordings: which is the recording electrode? *J Basic Clin Physiol Pharmacol*. 2016.
14. Gussak I, Chaitman BR, Kopecky SL and Nerbonne JM. Rapid ventricular repolarization in rodents: electrocardiographic manifestations, molecular mechanisms, and clinical insights. *J Electrocardiol*. 2000;33:159-170.
15. Fabritz L, Kirchhof P, Franz MR, Eckardt L, Mönnig G, Milberg P, Breithardt G and Haverkamp W. Prolonged action potential durations, increased dispersion of repolarization, and polymorphic ventricular tachycardia in a mouse model of proarrhythmia. *Basic Res Cardiol*. 2003;98:25-32.
16. Peng CK, Havlin S, Stanley HE and Goldberger AL. Quantification of scaling exponents and crossover phenomena in nonstationary heartbeat time series. *Chaos*. 1995;5:82-7.
17. Tse G, Tse V and Yeo JM. Ventricular anti-arrhythmic effects of heptanol in hypokalaemic, Langendorff-perfused mouse hearts. *Biomed Rep*. 2016;4:313-324.

18. Hinterseer M, Beckmann BM, Thomsen MB, Pfeufer A, Ulbrich M, Sinner MF, Perz S, Wichmann HE, Lengyel C, Schimpf R, Maier SK, Varro A, Vos MA, Steinbeck G and Kaab S. Usefulness of short-term variability of QT intervals as a predictor for electrical remodeling and proarrhythmia in patients with nonischemic heart failure. *Am J Cardiol*. 2010;106:216-20.
19. Tse G, Du Y, Hao G, Li KHC, Chan FYW, Liu T, Li G, Bazoukis G, Letsas KP, Wu WKK, Cheng SH and Wong WT. Quantification of Beat-To-Beat Variability of Action Potential Durations in Langendorff-Perfused Mouse Hearts. *Front Physiol*. 2018;9:1578.
20. Hekkanen JJ, Kentta TV, Haukilahti MAE, Rahola JT, Holmstrom L, Vahatalo J, Tulppo MP, Kiviniemi AM, Pakanen L, Ukkola OH, Junttila MJ, Huikuri HV and Perkiomaki JS. Increased Beat-to-Beat Variability of T-Wave Heterogeneity Measured From Standard 12-Lead Electrocardiogram Is Associated With Sudden Cardiac Death: A Case-Control Study. *Front Physiol*. 2020;11:1045.
21. Varkevisser R, Wijers SC, van der Heyden MA, Beekman JD, Meine M and Vos MA. Beat-to-beat variability of repolarization as a new biomarker for proarrhythmia in vivo. *Heart Rhythm*. 2012;9:1718-26.
22. Zaniboni M, Pollard AE, Yang L and Spitzer KW. Beat-to-beat repolarization variability in ventricular myocytes and its suppression by electrical coupling. *Am J Physiol Heart Circ Physiol*. 2000;278:H677-87.
23. Heijman J, Zaza A, Johnson DM, Rudy Y, Peeters RL, Volders PG and Westra RL. Determinants of beat-to-beat variability of repolarization duration in the canine ventricular myocyte: a computational analysis. *PLoS Comput Biol*. 2013;9:e1003202.
24. Zaniboni M, Cacciani F and Salvarani N. Temporal variability of repolarization in rat ventricular myocytes paced with time-varying frequencies. *Exp Physiol*. 2007;92:859-69.
25. Perkiomaki JS, Couderc JP, Daubert JP and Zareba W. Temporal complexity of repolarization and mortality in patients with implantable cardioverter defibrillators. *Pacing Clin Electrophysiol*. 2003;26:1931-6.
26. DeMazumder D, Limpitikul WB, Dorante M, Dey S, Mukhopadhyay B, Zhang Y, Moorman JR, Cheng A, Berger RD, Guallar E, Jones SR and Tomaselli GF. Entropy of cardiac repolarization predicts ventricular arrhythmias and mortality in patients receiving an implantable cardioverter-defibrillator for primary prevention of sudden death. *Europace*. 2016;18:1818-1828.
27. Banyasz T, Fulop L, Magyar J, Szentandrassy N, Varro A and Nanasi PP. Endocardial versus epicardial differences in L-type calcium current in canine ventricular myocytes studied by action potential voltage clamp. *Cardiovasc Res*. 2003;58:66-75.
28. Barandi L, Virag L, Jost N, Horvath Z, Koncz I, Papp R, Harmati G, Horvath B, Szentandrassy N, Banyasz T, Magyar J, Zaza A, Varro A and Nanasi PP. Reverse rate-dependent changes are determined by baseline action potential duration in mammalian and human ventricular preparations. *Basic Res Cardiol*. 2010;105:315-23.
29. Banyasz T, Horvath B, Virag L, Barandi L, Szentandrassy N, Harmati G, Magyar J, Marangoni S, Zaza A, Varro A and Nanasi PP. Reverse rate dependency is an intrinsic property of canine cardiac preparations. *Cardiovasc Res*. 2009;84:237-44.

Preprints (www.preprints.org) | NOT PEER-REVIEWED | Posted: 13 May 2022 doi:10.20944/preprints202205.0191.v1

Figures

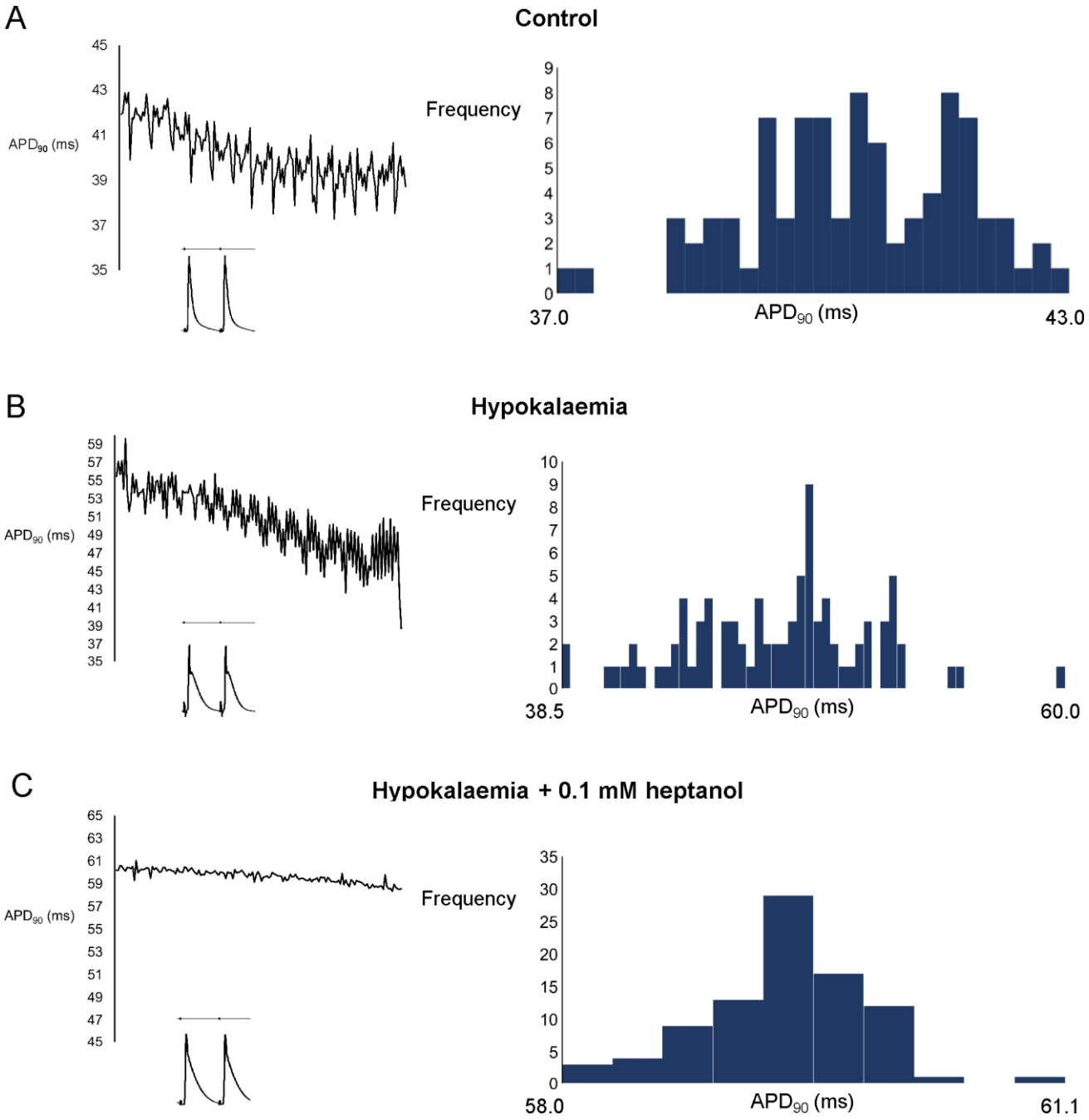

Figure 1. MAP traces, time series and histograms of APDs from a representative heart before (A) or after the application of experimental hypokalaemia (B) and hypokalaemia with 0.1 mM heptanol (C).

Preprints (www.preprints.org) | NOT PEER-REVIEWED | Posted: 13 May 2022 doi:10.20944/preprints202205.0191.v1

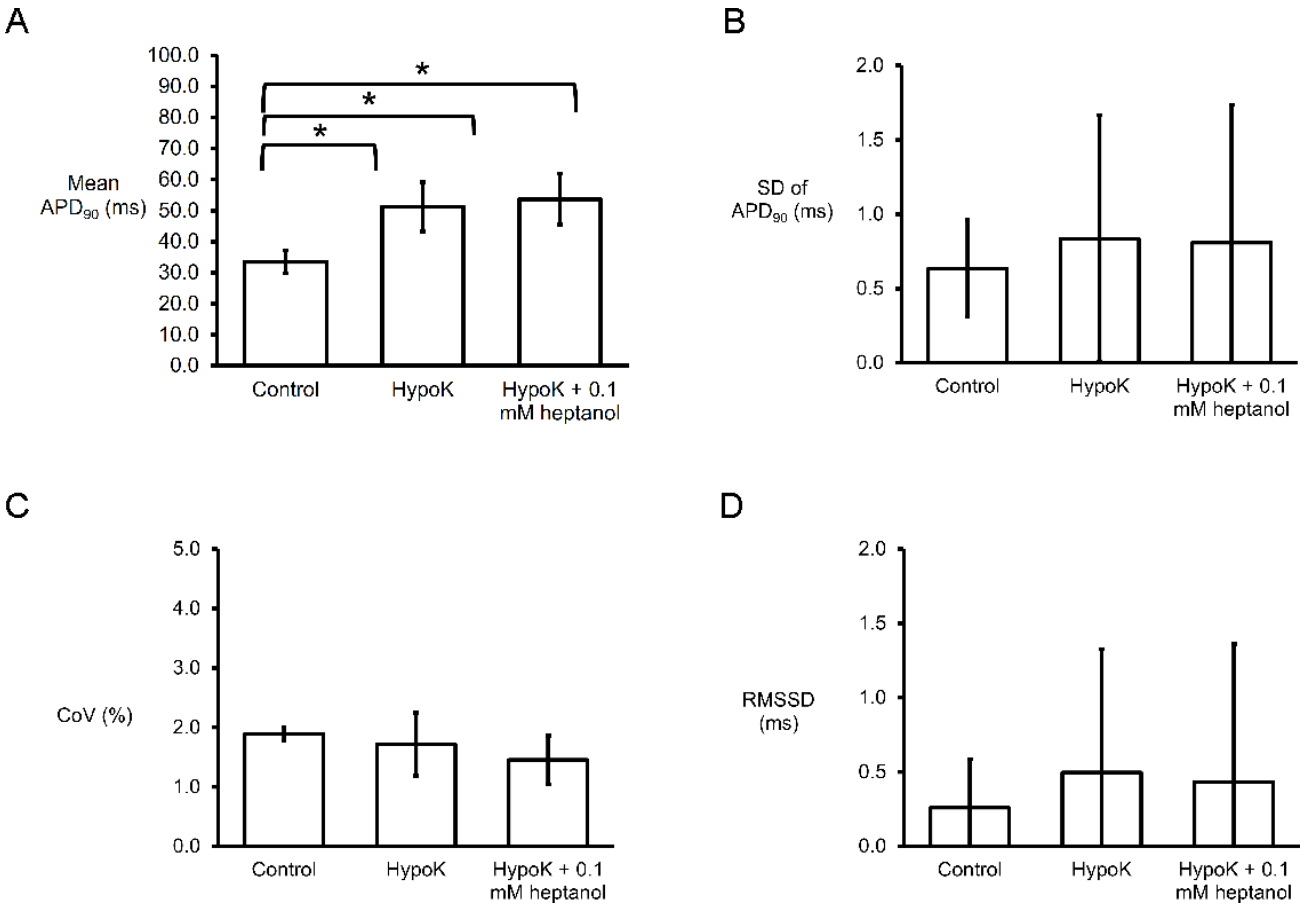

Figure 2. Time-domain analysis yielding mean APD (A), standard deviation (SD) of APDs (B), coefficient of variation (CoV) (C), and root mean square (RMS) of successive differences of APDs (D) (n = 6) (n = 7 hearts).

Preprints (www.preprints.org) | NOT PEER-REVIEWED | Posted: 13 May 2022 doi:10.20944/preprints202205.0191.v1

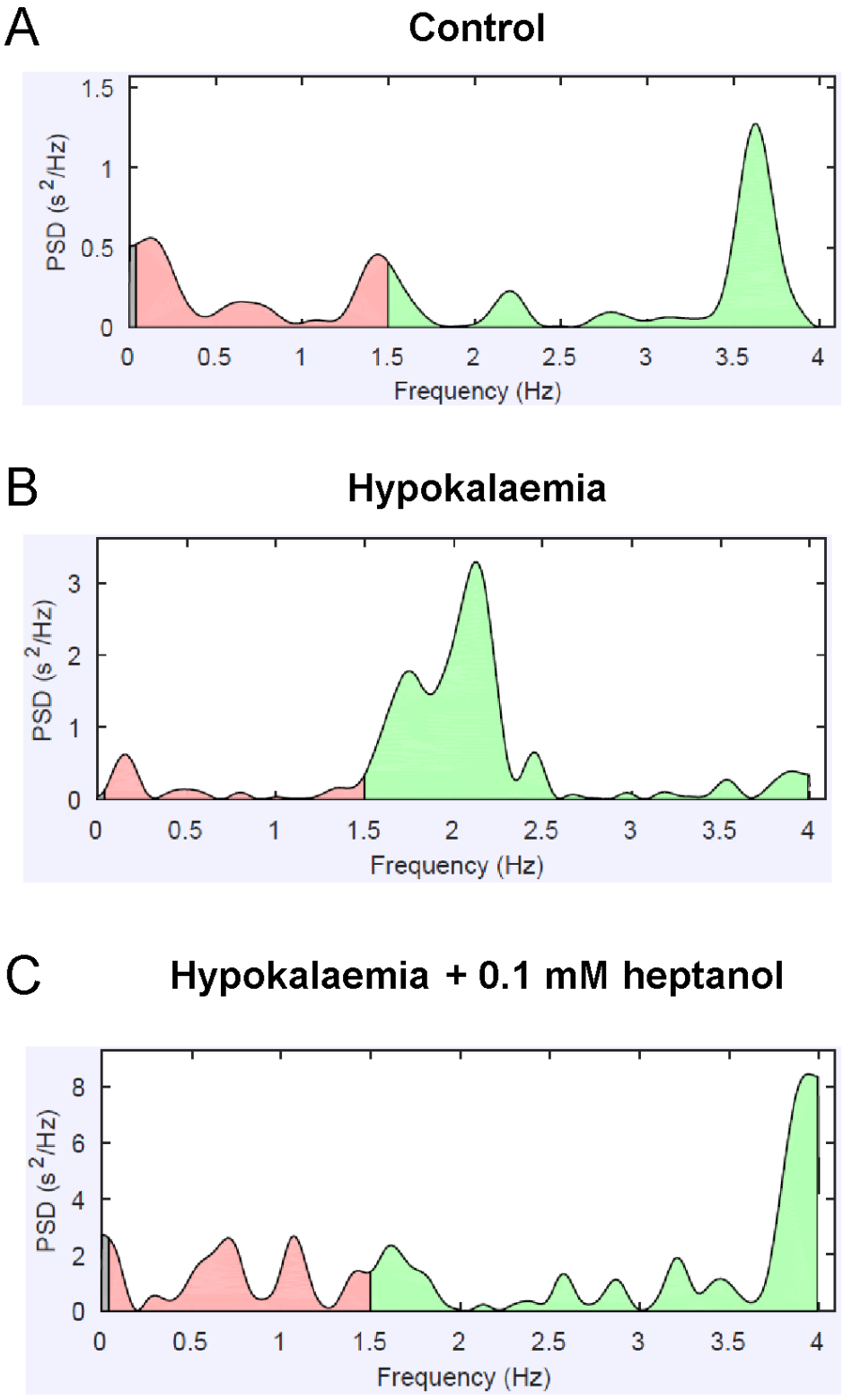

Figure 3. Examples of frequency spectra using the Fast Fourier Transform method from a representative heart before (A) or after the application of experimental hypokalaemia (B) and hypokalaemia with 0.1 mM heptanol (C).

Preprints (www.preprints.org) | NOT PEER-REVIEWED | Posted: 13 May 2022 doi:10.20944/preprints202205.0191.v1

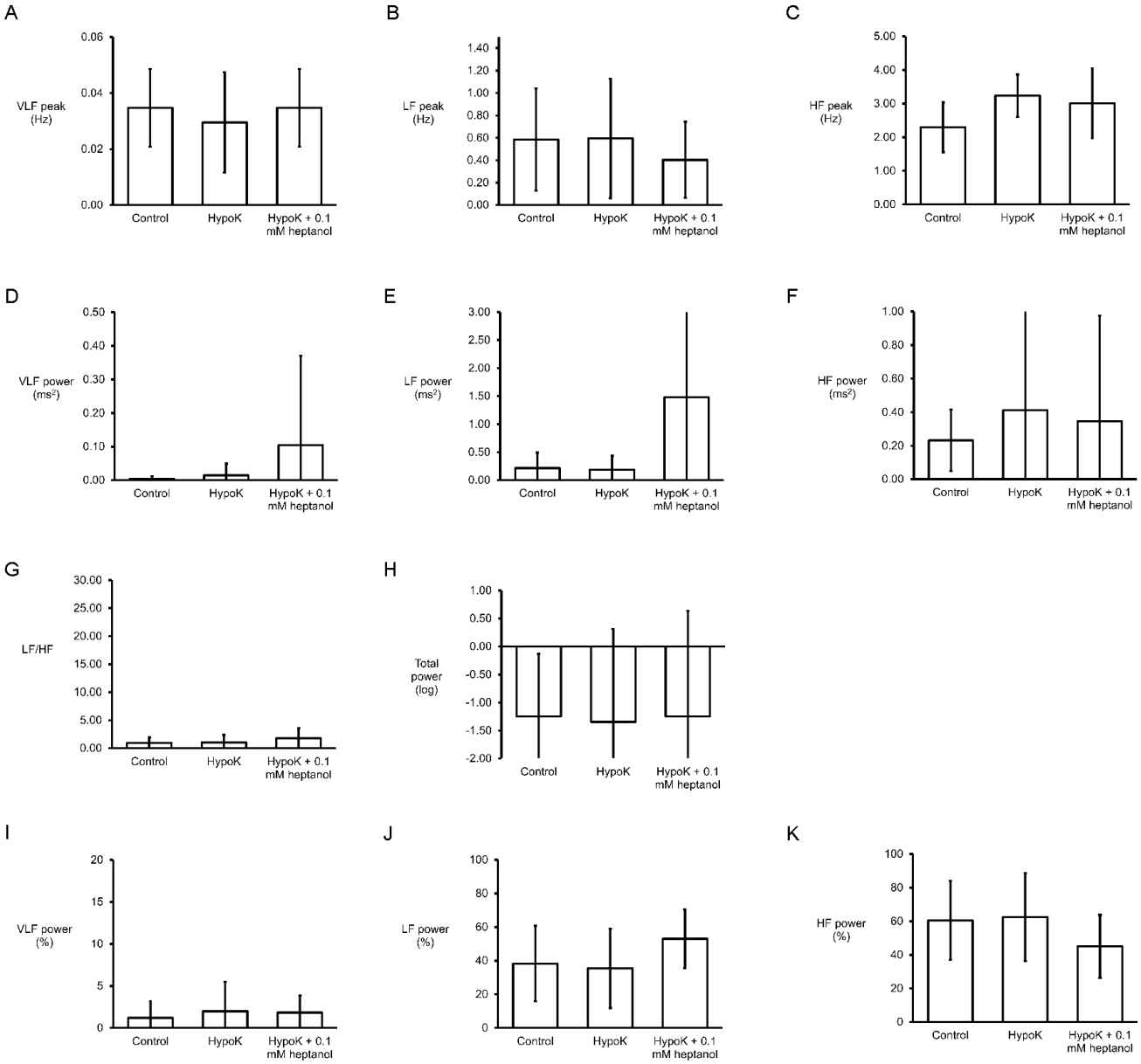

Figure 4. Peaks for very low- (A), low- (B) and high-frequency (C), their corresponding powers (D, E and F), low-frequency to high-frequency ratio (G) and total power (H). The percentage powers for very low- (I), low- (J) and high-frequency (K) bands (n = 7 hearts).

Preprints (www.preprints.org) | NOT PEER-REVIEWED | Posted: 13 May 2022 doi:10.20944/preprints202205.0191.v1

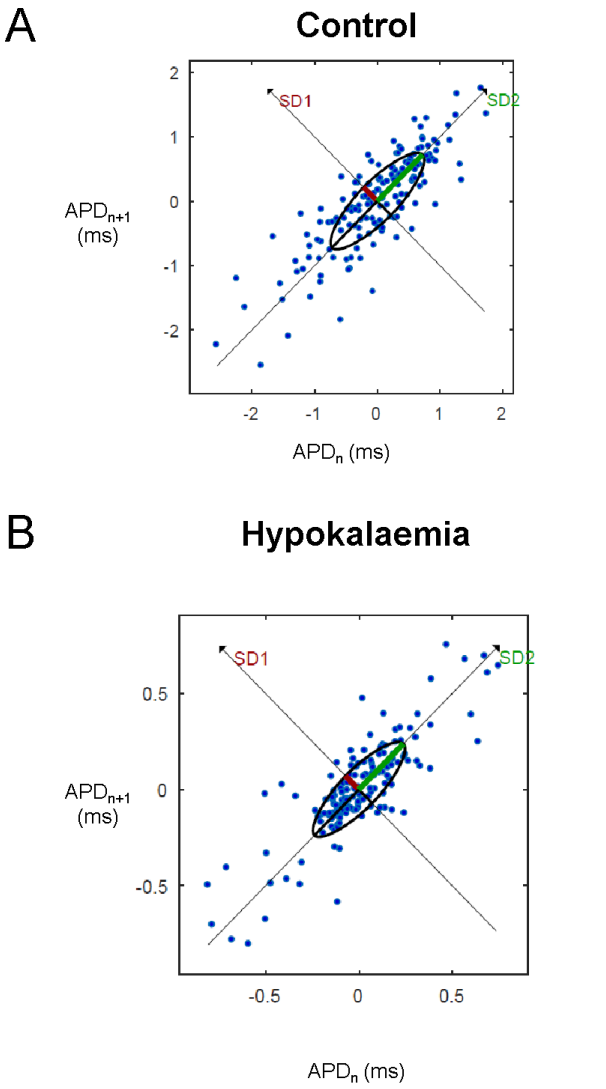

Figure 5. Representative Poincaré plots of APD_{n+1} against APD_n with SD along the line-of-identity (SD1) and SD perpendicular to the line-of-identity (SD2) before (A) or after the application of experimental hypokalaemia (B) and hypokalaemia with 0.1 mM heptanol (C) (n = 7 hearts).

Preprints (www.preprints.org) | NOT PEER-REVIEWED | Posted: 13 May 2022 doi:10.20944/preprints202205.0191.v1

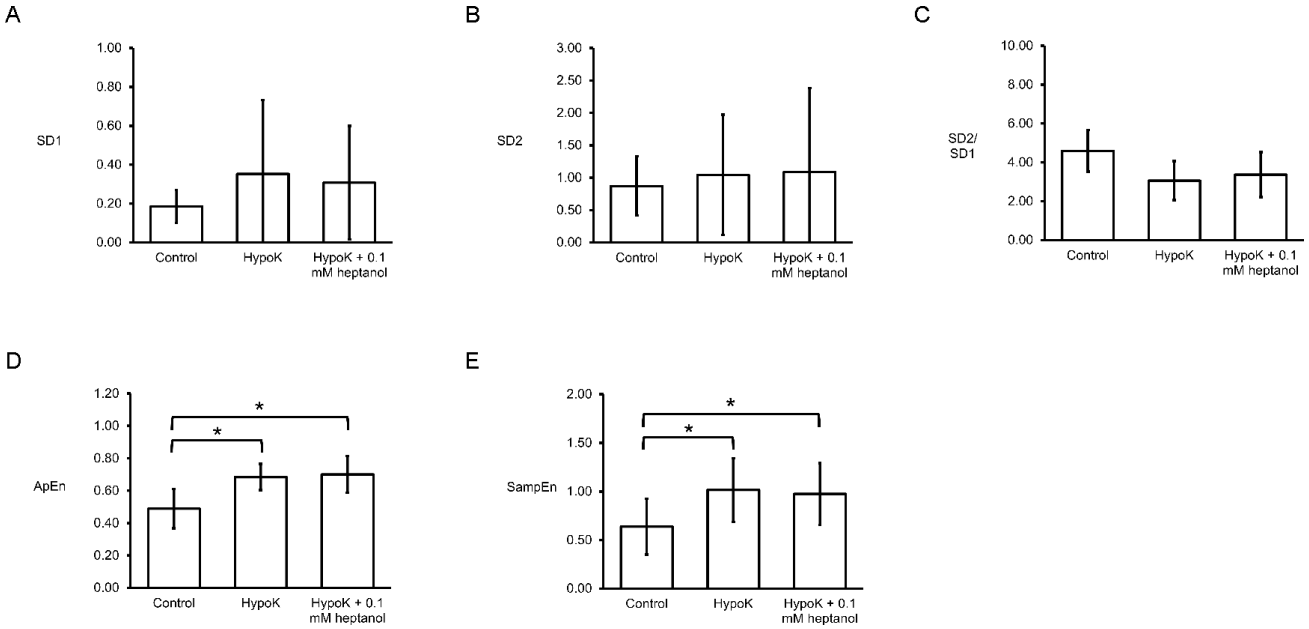

Figure 6. Bar charts plotting SD perpendicular to the line-of-identity (SD1) (A), SD along the line-of-identity (SD2) (B), SD2/SD1 ratio (C), the approximate entropy (D) and the sample entropy (E) (n = 7 hearts).

Preprints (www.preprints.org) | NOT PEER-REVIEWED | Posted: 13 May 2022 doi:10.20944/preprints202205.0191.v1

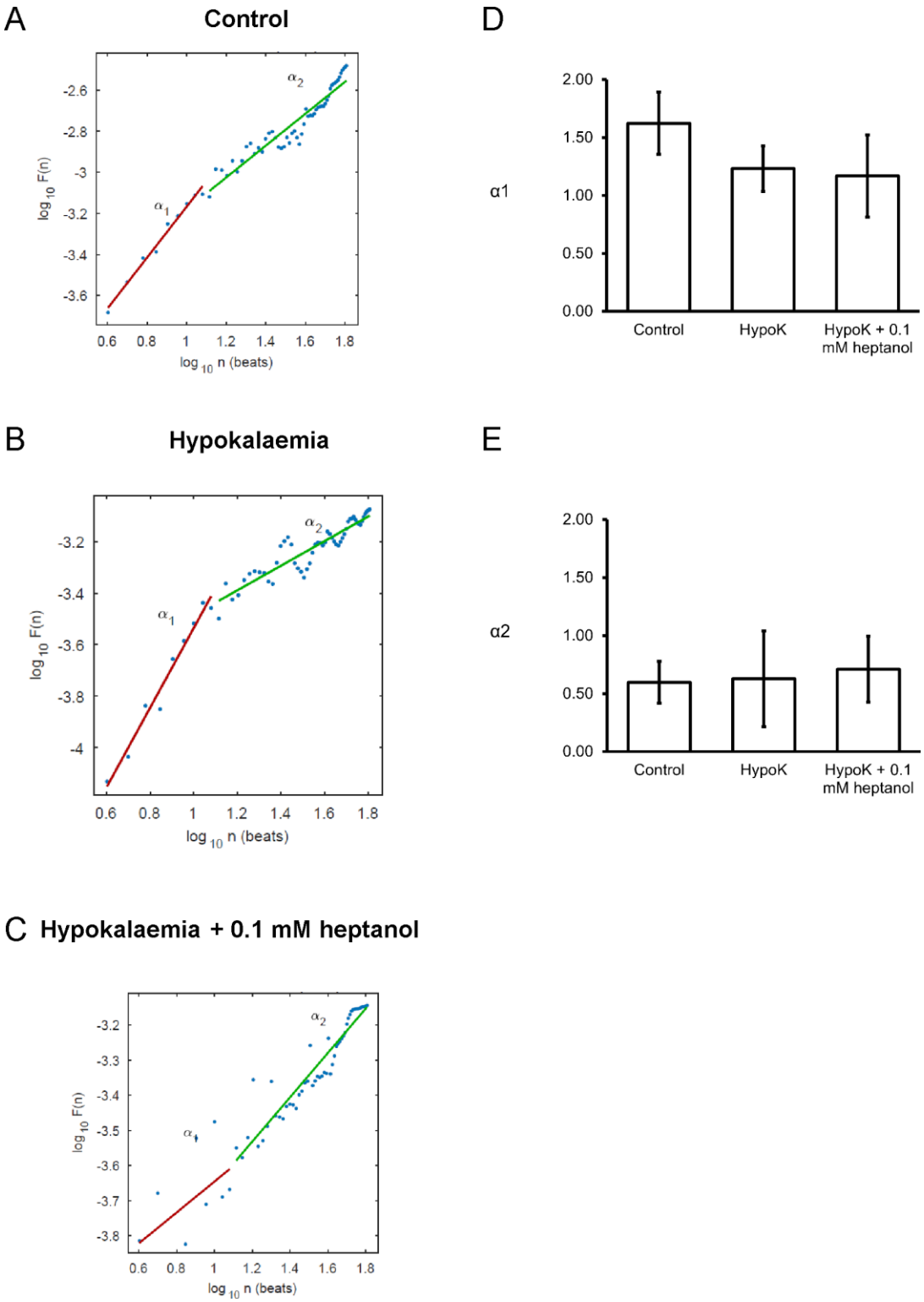

Figure 7. Detrended fluctuation analysis plots expressing detrended fluctuations F(n) as a function of n in a log-log scale before (A) or after the application of experimental hypokalaemia (B) and hypokalaemia with 0.1 mM heptanol (C). Short-term (D) and long-term (E) fluctuation slopes (n = 7 hearts).